

## **APPENDIX B**

## **1. DESCRIPTION OF FRACTURED WATER INJECTION MODEL [2]**

The purpose of this computer program is to provide via simulation an estimate of lateral and vertical extension of waterflood-induced fractures (both for clean water and produced water injection), of vertical fracture (non-)confinement to target injection zones, of well injectivity, and of the shape and extent of flooded zones. It was developed by merging [1] existing fracturing/CRI [2] and waterflooding [3] software packages during the late nineties of last century into a combined model suited to simulate both hydraulic fracturing (HF), Cuttings Re-Injection (CRI) and Water Injection (WI).

Applications of this program throughout the years have been mainly in the arena of water injection for waterflooding, for reservoir voidage replacement and for (contaminated) water disposal [4-20]. In most of these applications, water injection simulations were carried out to assess issues around fracture containment, sweep and injectivity.

In many waterfloods, fractured water injectors are a common feature. Unintended fracturing in water injectors may occur owing to thermal effects (particularly in offshore areas) or due to pore plugging by impurities in the injection water. Intentional fracturing may be an integral part of the field development plan, since the increased injection potential may enable a significant reduction in the number of injector wells drilled. Furthermore, as a result of fracturing, water purity requirements may be relaxed providing a significant reduction in facilities costs, especially offshore. However, once fracture lengths reach a significant fraction of the well spacing they can have a significant influence on sweep efficiency. Furthermore, if the fracture does not extend over the full height of the formation, non-uniform sweep in the vertical sense may be encountered which may alter field development plans. Finally, intended or unintended fracturing may lead to out-of-zone growth, particularly when injection rates significantly exceed leakoff rates owing to low formation permeabilities and/or limited disposal storage capacity of the target injection zones. Therefore, the accurate prediction of fracture length and height is required.

Our WI/CRI injection model computes fracture dimensions, well injectivities, and flood front displacements for water injection under induced fracturing conditions. This applies both to produced water injection and to clean (e.g. sea-)water injection.

## 2. VALIDATIONS

### 2.1. Validations against other simulators

Extensive validation [2] was carried out of our fractured WI/CRI model against a number of published results of other fracture simulators, both with a gridded fracture shape [BEM model, 21] and with fixed shapes [22-25]. These validations were carried out on the SPE benchmark set for hydraulic fracture simulators which consisted of 17 cases (called A-O, II and VI) covering contained and uncontained fracture growth (with and without gradient), low and 'high' leak-off, and Newtonian / non-Newtonian injection fluids. Results obtained were overall close to results obtained by the other models and well within the spread of the results [2]. Additional validations were carried out using the well-known HF stimulation field case of SFE-3 that was executed by the US Gas Research Institute in the early nineties [2].

For cuttings re-injection (CRI) applications the capability to simulate 'uncontained' hydraulic fracture growth is essential. Therefore, we also did benchmarks against other models for the situations of uncontained growth in the presence of an in-situ stress gradient, with or without a 'negative' stress contrast (i.e. growth from a higher stress into a lower stress zone).

An example of CRI is shown in Fig. 1 (Northern North Sea, UK sector) [2]. Clearly, our fractured WI/CRI model and the BEM model used in this study yield the highest degree of uncontained upward fracture growth. The other models show far less upward growth. This is a general shortcoming of many of the commercial hydraulic fracture simulation models, which were mostly designed for typical US-hydraulic fracture stimulation settings (strongly contained hydraulic fractures).

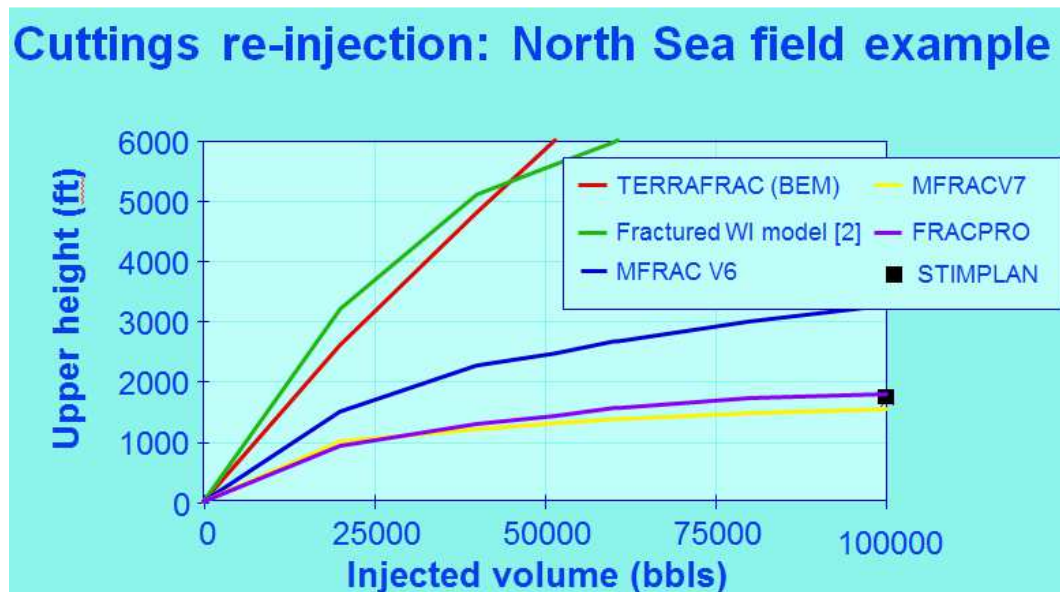


Figure 1. Comparison of different fracture simulators for CRI field example in the North Sea

An example for hydraulic fracture growth in the presence of negative stress contrasts is shown in figure 2 below. As can be seen on the left, the BEM model predicts a fracture with lengthwise 'bulging' in the lower stress zones whilst our fractured WI/CRI model has a fixed shape of two half-ellipses that more or less (on average) follow the contours of the BEM model. In the case on the right, the BEM model also predicts an elliptically shaped fracture, because in this case the impact of the negative stress contrasts is lower as a result of the high net pressure.

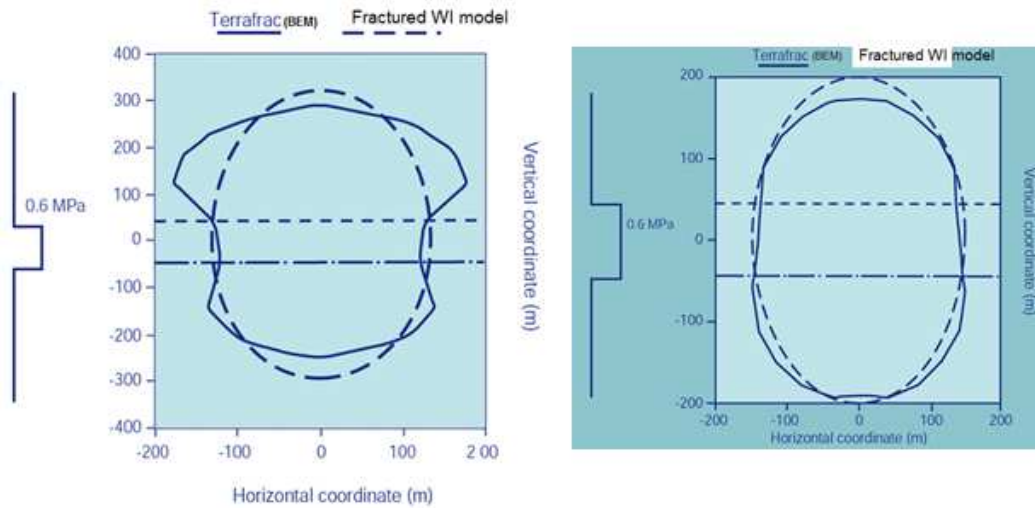


Figure 2. Hydraulic fracture growth from a higher stress zone into a lower stress zone, in the presence of low (left) and high (right) net pressures.

Finally, figure 3 shows the comparisons for a massive hydraulic fracture (MHF) treatment for the NAM offshore the Netherlands [2]. In this case, modeling was required in order to determine the optimum injection depth, and subsequently compute the optimized pump (proppant schedule).

### MHF treatment NAM (Netherlands)

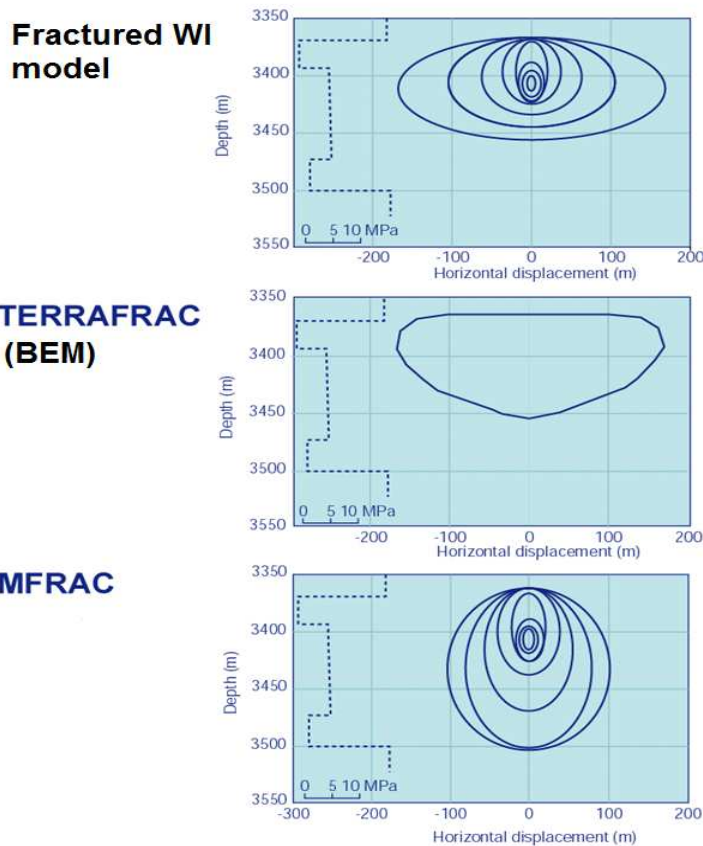


Figure 3: Comparison of WI/CRI fracture model with TERRAFRAC (BEM) and MFRAC for NAM offshore MHF.

## 2.2. Validations against field observations

Our fractured WI/CRI model has been applied to numerous field cases, especially for waterflooding and water injection disposal purposes. Comparison with field observations was always indirectly, e.g. by successful pump schedules based on HF designs [e.g. 2, see above], PLT's in water injectors [5], pressure transient testing [e.g.12-16], fracture breakthrough (or the absence thereof) in nearby producers (waterflooding) [12], in-well tiltmeter measurements [14], temperature logging [16,19, 20], and continuous monitoring plus history matching of observed injection rates and pressures.

### 2.2.1. Pattern waterflood in Oman: Field development [12]

A pattern waterflood was designed with the intent to inject highly contaminated production water into an oil reservoir with a fairly low reservoir fluid mobility. For such situations, pattern floods with close well spacing are ideally suited to optimize recovery. However, at the same time reasonable injection rates are only achievable when some degree of induced fracturing around the injector is allowed. Obviously this obliges the operator to consider an optimal operational scheme such that on one hand he profits from good injectivity whilst on the other hand, the induced fractures do not grow excessively large, either into the overlying reservoir caprock or into adjacent producer wells.

In order to gain experience with induced fracturing and use this to aid in an optimum field development program, a trial with a five-spot pattern flood was carried out. The layout is shown in figure 4 below.

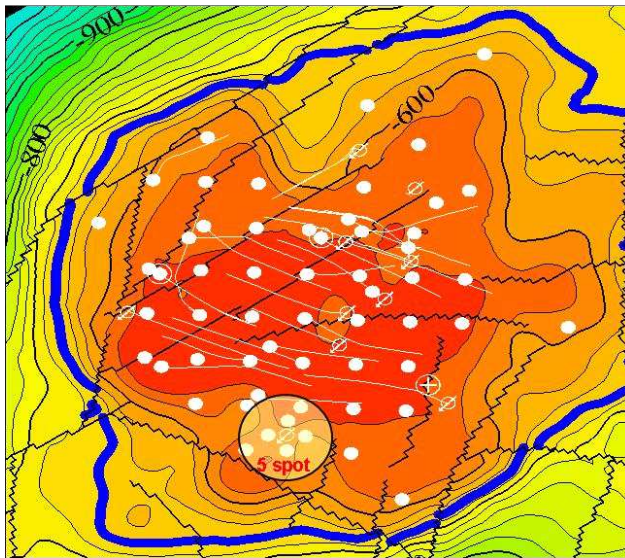


Figure 4: Sub-surface map of reservoir highlighting the area of 5-spot inverted pilot in the south of the field [12].

The pilot was carried out as a step-rate test with long-duration steps in order to also observe the impact on production in neighboring producers. The plot in figure 5 shows the injection rate and duration of each step, and also the computed fracture length by our WI/CRI simulator (coupled to a reservoir simulator [15] to capture the impact on the production rates of nearby wells). As can be seen, for low injection rate (below ca 150-200 m<sup>3</sup>/d), no appreciable fractures are formed. However, as soon as one exceeds the 200 m<sup>3</sup>/d, fractures grow with lengths that “rapidly” increase with increasing injection rate. At 400 m<sup>3</sup>/d injection rate, water breakthrough was seen in adjacent producers. This is in line with the simulations in the sense that the computed fracture length (150-200 m) becomes equal to the well spacing.

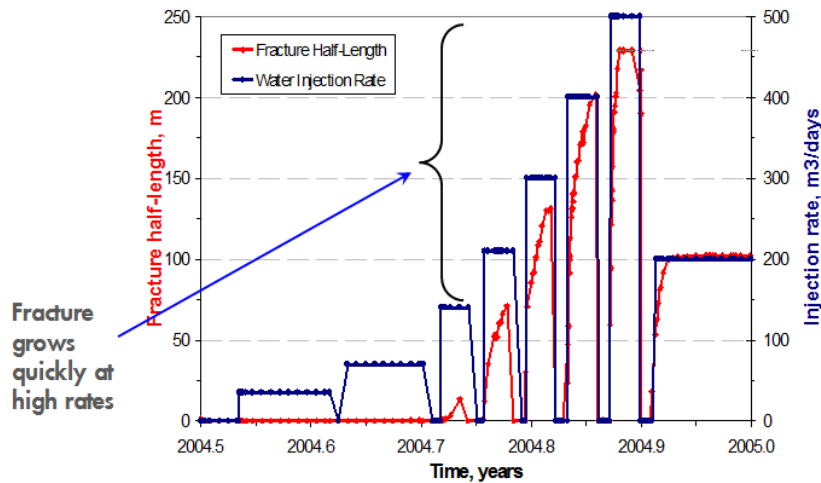


Figure 5: Injection scheme during 5-spot trial plus computed fracture lengths

An important implication of this study was that the size of induced fractures could be kept in check by properly managing the injection rates over the field life. Particularly, it turned out that initially when the reservoir is filled with low-mobility oil, injection rates should be kept at a fairly low level. When gradually increasingly more oil is replaced by higher mobility (injected) water, higher injection rates can be applied without the risk of excessive fracturing.

### 2.2.2. Pattern waterflood onshore Russia (West Siberia): Pattern infill [16]

In this field, a pattern waterflood using low-quality injection water in a light oil field had been already ongoing for some time. The issue at stake here was that pattern infill drill campaigns were being planned and the question was how to manage the induced fractures by an appropriate choice of injection water quality and injection rate, see figure 5.

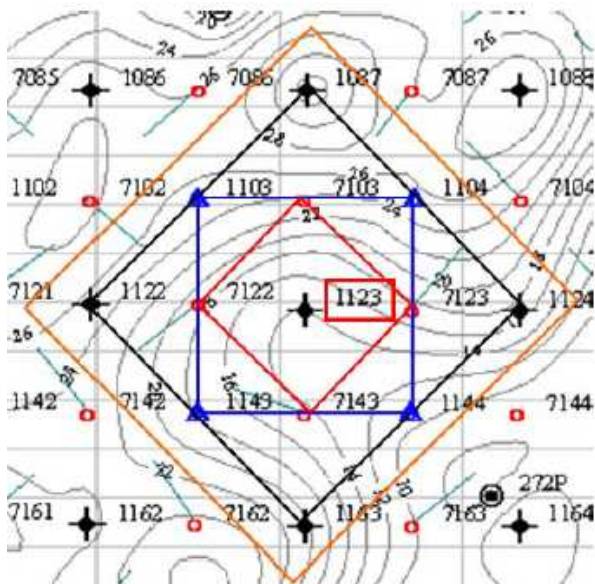


Figure 5: Pattern waterflood lay-out for field in Russia

In this case, fracture dimensions around the injector (no 1123) were monitored on a regular basis by means of pressure fall-off testing ( $\rightarrow$  fracture length, height) and temperature logging (fracture height). Examples of these measurements are shown in figures 6 and 7 below.

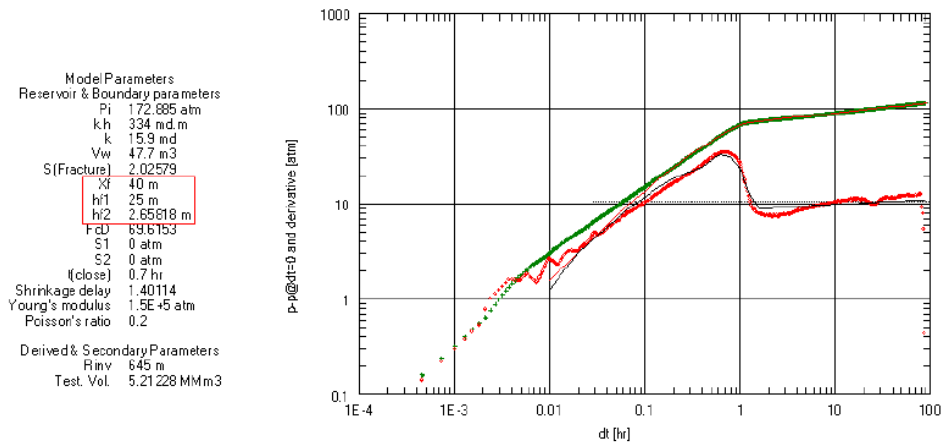


Figure 6: Example of pressure fall-off test and its interpretation

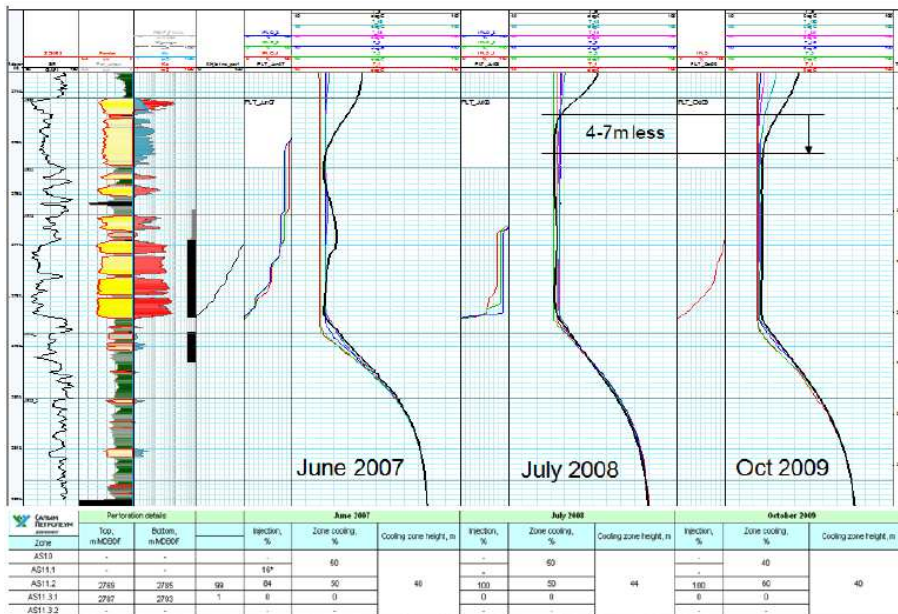


Figure 7: Examples of temperature logs over time and their interpretation

The plot in figure 8 shows the computed fracture length and height by our WI/CRI simulator, in comparison with the fracture lengths as interpreted from pressure fall-off tests. Agreement is reasonable (especially in view of the large data uncertainty), although it appears that the WI/CRI simulator is somewhat on the conservative side at later times.

The results as shown (plus many sensitivities) formed the basis for a decision on infill drilling (pattern, spacing), future injection rate and injection water quality.

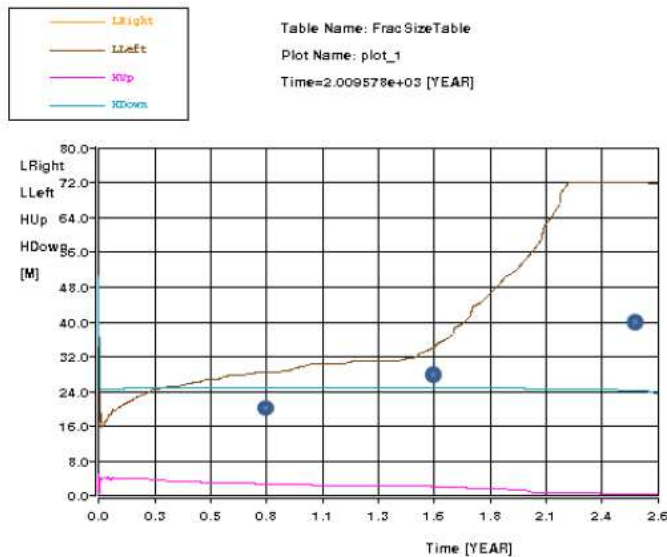


Figure 8. Fracture length growth map of historical injection results : computed versus interpreted from pressure fall-off tests.

2.2.3. Large-scale produced water disposal (Oman): Risk of fracture containment [5,14]

Very large-scale produced water injection disposal was pioneered in the late nineties [5]. High volumes of contaminated production water had to be re-injected. A suitable injection horizon was found. However, there was a non-negligible risk that the induced fractures would grow through the overlying caprock shale into potable water-bearing shallow formations.

The basic lay-out is shown in figure 10. Unfiltered produced water is injected into the far flank of the deep formation. This is a fairly homogeneous, medium-permeability (approx. 300mD), medium-strength sandstone with a thickness of several hundreds of metres. The caprock (8 – 18m thick) at approx. 1000 m TVD, provides a sealing shale layer with extensive lateral extent. The carbonate formation above the shale layer is in contact with shallow aquifers, so it is essential that injected production water does not penetrate upwards through the caprock shale. As indicated in the figure, this requirement had an impact on the optimum injection depth.

Figure 9 shows the history-matched injection rates and pressures using the fractured WI/CRI-model, whilst the computed induced fracture is shown in Fig. 10. Its is clear from this figure that the initially planned injection depth was inappropriate. Based on this study, the injection depths for all planned water injection disposal wells were moved down by about 300 m.

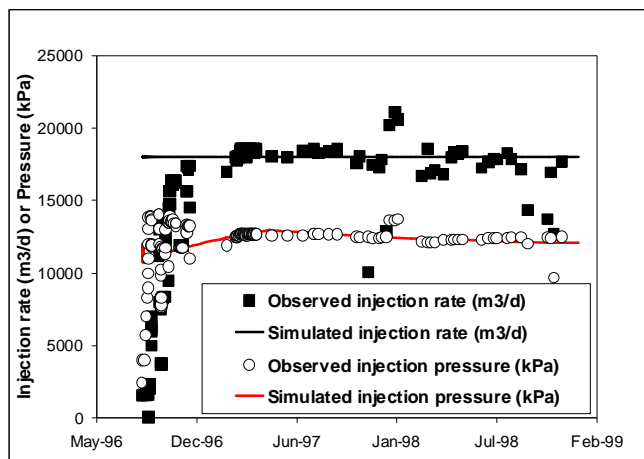


Fig. 9 – Observed and simulated historical injection performance for one of the pilot wells.



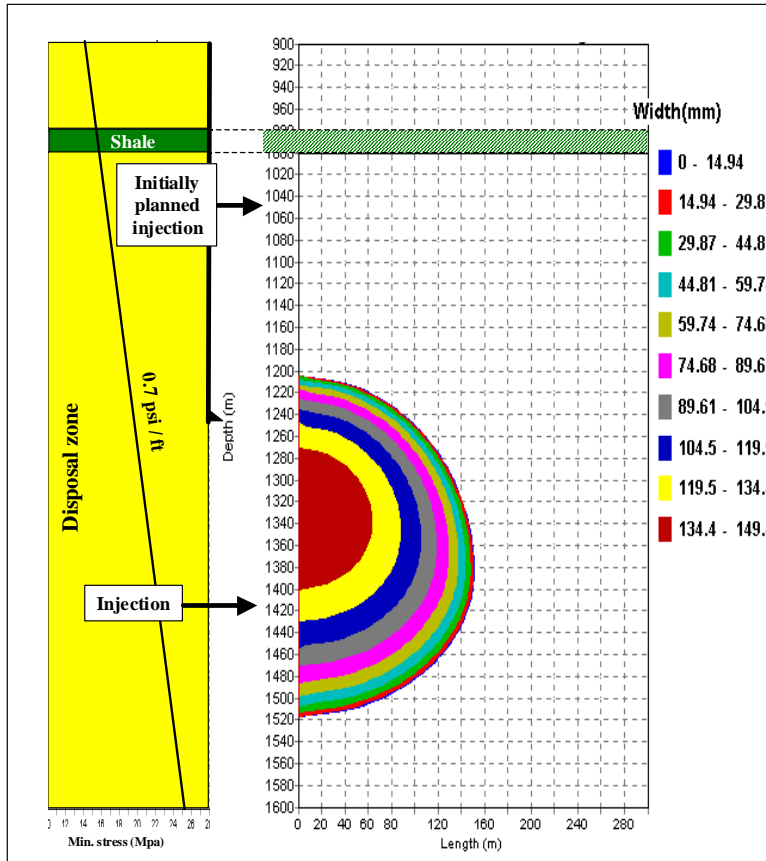


Fig. 10 – Overview of subsurface injection disposal horizons. Also indicated are casing shoe and induced fracture after 20 years of injection for one of the injectors [5].

After the injection disposal wells were on-stream, a number of different surveillance techniques was tried to validate / calibrate the fracture simulations (especially with respect to upward fracture height), but the initial results were fairly inconclusive [5]. Early 2007, the technique of downhole tiltmeters was successfully applied in a trial to measure induced fracture height. This technique has been well-proven for propped fracture applications in tight rocks but applications in medium- to high-permeability waterflood applications had been limited. Because none of the disposal wells had nearby observation wells, it was decided to use the technique of “treatment well tilt” in which the tiltmeters are deployed in the injection well itself. This allows for “optimal” measurement of fracture height (maximum tilt signal), although fracture length cannot be measured in this way. The tiltmeter measurements were combined with pressure fall-off tests after each injection cycle to interpret fracture lengths.

Figure 11 shows the injection / shut-in sequence during the tiltmeter trial. From the horizontal scale of this graph it can be seen that the well had already been injecting ca 4 years prior to the trial. Figure 12 shows an example of a raw tiltmeter signal alongside an “ideal” signal for the case of one planar vertical fracture. As can be seen, ideally the locations of fracture top and bottom are identified from the maxima in the tilt signal, but in our case four (instead of two) of such maxima were observed, leading to some ambiguity in the interpretation of fracture height. In the interpreted results we took this into account by indicating a range for fracture height rather than one value. Finally, Figure 13 shows an example of one of the injection fall-off test results. These results show a pronounced storage-dominated flow period, which is indicative of a large induced fracture [25].

Figure 14 shows a summary of the interpreted fracture heights and lengths from tiltmeter and fall-off tests, together with the fracture dimensions as computed by our WI/CRI fracture simulator, for 4 years injection history, plus the injection cycles as depicted in Fig 11. During the latter of these injection cycles, no reliable tiltmeter signals could be obtained owing to their detachment from the borehole wall (casing). As can be seen from Fig. 14, the computed and measured results are in fairly good agreement, especially when considering the large uncertainties both in the measurements and computations.

Fig. 14 also shows that the maximum total fracture height during the injection trial is far less than the 300 m that was based on earlier simulations (see discussion above, and figure 10). However, this turned out to be mainly the result of two essential differences between the trial on one hand and continuous injection on the other hand: (1) During continuous injection, rates of ca 20,000 m<sup>3</sup>/d are applied, which was never achieved during the trial, and (2) the limited duration of the trial resulted in induced fractures which were still growing under the influence of transient pressure build-up in the reservoir. Without these two effects, induced fractures are likely to grow towards ca 300 m height, as is illustrated in Fig. 15 which shows the computed result of continuous injection for 4 years at 20,000 m<sup>3</sup>/d.

Summarizing the above discussion, the simulated sizes of the induced fracture were confirmed by surveillance data (tiltmeter, fall-off), endorsing the policy of perforating water disposal wells at least 300m below the caprock.

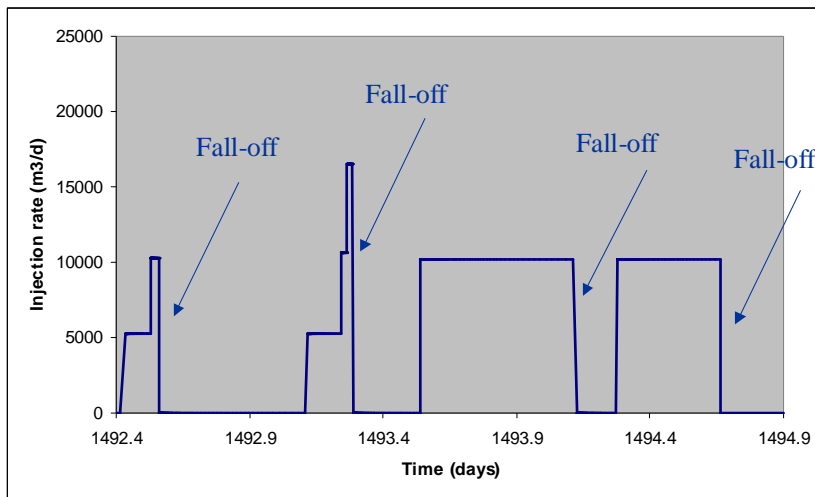


Fig. 11. Oman water disposal well: Injection cycles of tilmeter test

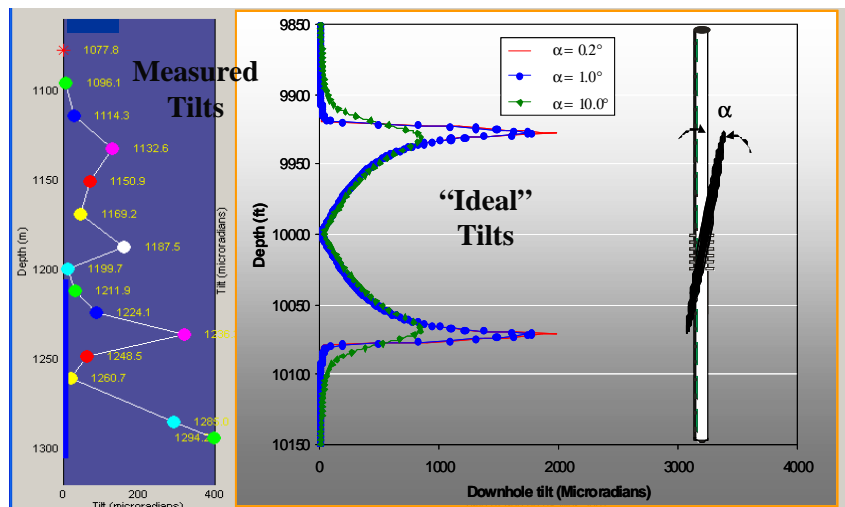


Fig. 12. Oman water disposal well: Example of tilmeter data

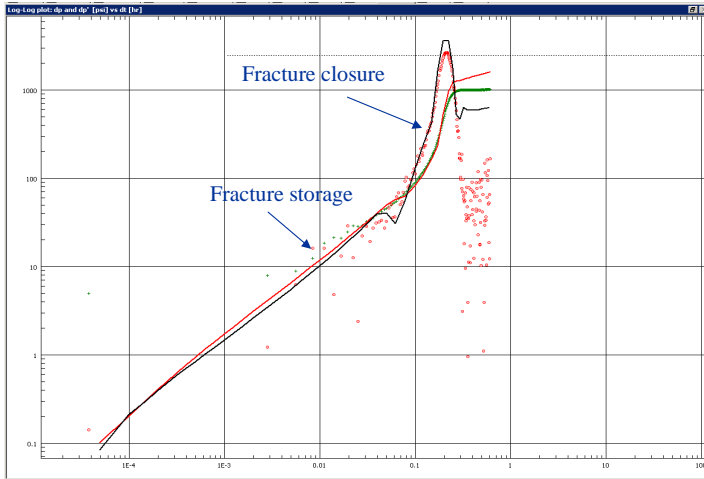


Fig. 13. Oman water disposal well: Example of pressure fall-off test data

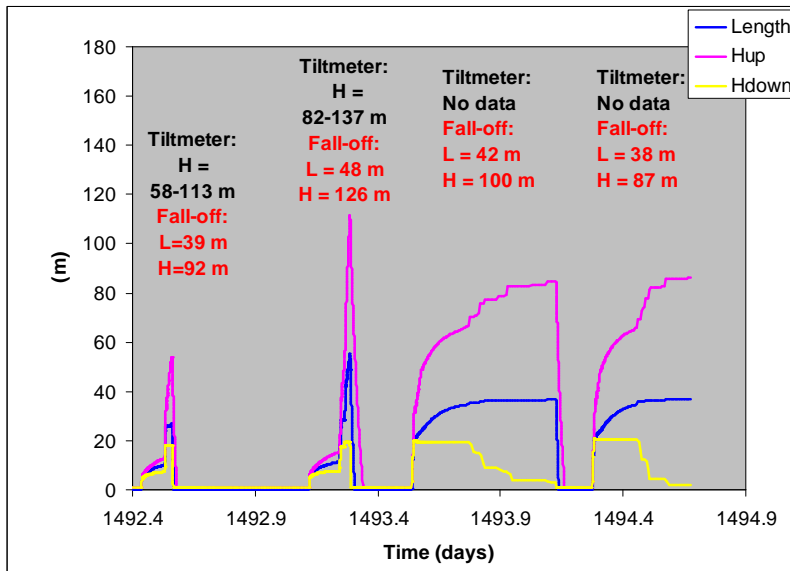


Fig. 14. Oman water disposal well: Summary of tiltmeter test results. Colored curves represent computed results: Length (L), Hup (=upward fracture height), and Hdown (downwards fracture height).  $H = \text{total fracture height} = \text{Hup} + \text{Hdown}$ .

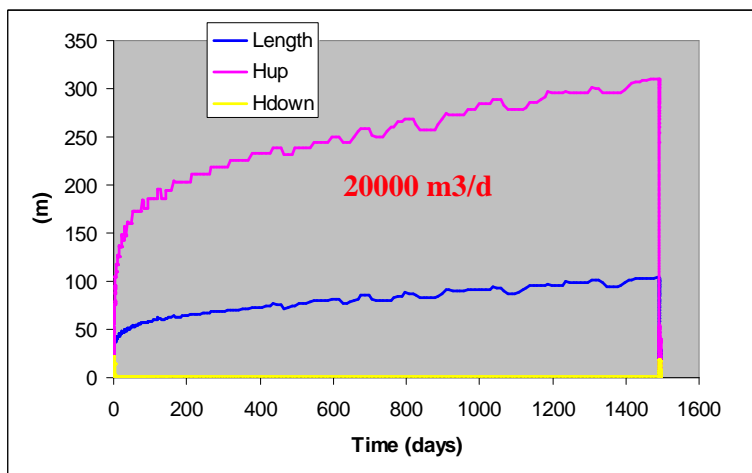


Fig. 15. Oman water disposal well: Computed fracture dimensions for high-rate disposal injection

### **2.3. Conclusions from validations.**

The above paragraphs have illustrated a number of cases where the performance of our WI/CRI fracture simulator was validated both against other simulators and against field data. Overall, the agreement is acceptable, especially in view of the large input data uncertainties for field cases.

There are a number of important points that one has to bear in mind when using this model (or other models with similar functionality) for field applications. First, because of limited data and limited understanding of the subsurface, simulation results can vary widely. Therefore, regular surveillance / monitoring will always be a requirement. Such surveillance results can be history-matched and subsequently used to update the input data. Secondly, it is vital that the user has a proper qualitative 'physical' understanding of the results from a simulator – i.e. there should be no using hydraulic fracture simulators in 'black box' mode. Trying to understand the results from hydraulic fracture simulators can often be quite challenging, but it does help to track deficiencies in the input data, in the understanding of the subsurface, and/or the hydraulic fracture simulator itself.

## REFERENCES

1. G.Gheissary, P.A. Fokker, P.J.P. Egberts, F.J.T. Floris, G. Sommerauer and C.J. Kenter. Simulation of Fractures Induced by Produced Water Re-Injection in a Multi-Layer Reservoir. SPE 54735, presented at the SPE/ISRM Eurock '98 held in Trondheim, Norway, 8–10 July 1998.
2. P.J. van den Hoek. New 3D model for optimised design of hydraulic fractures and simulation of drill cuttings re-injection. SPE 26679, presented at SPE Offshore Europe, Aberdeen (1993).
3. Koning, E.J.L., Waterflooding under fracturing conditions, Ph.D. Thesis, Technical University of Delft, 1988.
4. Van den Hoek, P.J., Matsuura, T., De Kroon, M., and Gheissary, G.: "Simulation of Produced Water Injection Under Fracturing Conditions", SPE Prod. & Facilities 14 (3) August 1999, p. 166-176.
5. P.J. van den Hoek, G. Sommerauer, L. Nnabuihe, and D. Munro. Large-scale produced water re-injection under fracturing conditions in Oman. SPE 87267 (ADIPEC 0963), presented at Abu Dhabi Petr. Conference (2000).
6. P.J. van den Hoek, Z.I. Khatib, and G.J. Siemers. Causes of Injectivity Problems During Fractured Water Disposal and Their Remediation. SPE 74416, presented at SPE IPCEM, Villahermosa (2002).
7. M. Bai, S. Green, and P.J. van den Hoek. A parametric analysis of deep injection for waster disposal using a 3-D hydraulic fracture simulator (presented at NARMS conference, Toronto, 2002).
8. J.C. Noirot, P.J. van den Hoek, Dirk Zwarts, Hans Petter Bjoerndal, SPE, Rik Drenth, R. Al Masfry, B. Wassing, J. Saebby, M. Masoori, and A. Zarafi. Water Injection and Water Flooding Under Fracturing Conditions. SPE 81462, presented at SPE MEOS, Bahrain (2003).
9. S. Sathyamoorthy, P. Priyandoko, K.B. Flatval, A. Bulang, P.J. van den Hoek, and Y. Qiu. Radical Approach to Water Injection Scheme for Barton. SPE 84885, presented at SPE improved oil recovery conference in Asia Pacific, Kuala Lumpur (2003).
10. K.I. Ojukwu and P.J. van den Hoek. A New Way to Diagnose Injectivity Decline During Fractured Water Injection By Modifying Conventional Hall Analysis. SPE 89376, presented at SPE/DOE conference on improved oil recovery, Tulsa (2004).
11. B. Hustedt, Y. Qiu, D. Zwarts, and P.J. van den Hoek. Modeling Water-Injection Induced Fractures in Reservoir Simulation. SPE 95726, presented at SPE ATCE, Dallas (2005).
12. J. Sæby, H.P. Bjørndal, and P.J. van den Hoek. Managed Induced Fracturing Improves Waterflood Performance in South Oman. IPTC-10843, presented at IPTC, Doha (2005).
13. Hustedt, B., Qiu, Y., Zwarts, D., van Schijndel, L., and P.J. van den Hoek. The Impact of Water-Injection Induced Fractures on Reservoir Flow Dynamics: First Applications of a New Simulation Strategy. IPTC-10689, presented at IPTC, Doha (2005).
14. P.J. van den Hoek, B. Hustedt, M. Sobera, H. Mahani, R.A. Masfry, J. Snippe and D. Zwarts. Dynamic Induced Fractures in Waterfloods and EOR, SPE 115204, presented at the 2008 SPE Russian Oil & Gas Technical Conference and Exhibition held in Moscow, Russia, 28–30 October 2008.
15. B. Hustedt, D. Zwarts, H.-P. Bjoerndal, R. Masfry, and P.J. van den Hoek. Induced Fracturing in Reservoir Simulations: Application of a New Coupled Simulator to

- Waterflooding Field Examples. SPE Reservoir Evaluation & Engineering Journal, Vol. 11 (June 2008), p. 569-576.
16. A. Aniskin, I. Chmuzh, R. Sakhibgareev. Waterflood induced fracturing in the West Salym field. SPE 136560, presented at the 210 SPE Russian Oil & Gas Technical Conference and Exhibition held in Moscow, Russia, 26-28 October 2010.
  17. Van den Hoek, P.J., Al-Masfry, R., Zwarts, D., Jansen, J.D., Hustedt, B., and Van Schijndel, L. Waterflooding Under Dynamic Induced Fractures: Reservoir Management and Optimization of Fractured Waterfloods. SPE Reservoir Evaluation & Engineering Journal, October 2009, p.671-682.
  18. M. Khodaverdian, T.G. Sorop, P.J. van den Hoek, S.Sathyamoorthy and E. Okoh. Injectivity and fracturing in unconsolidated sand reservoirs: Waterflooding case study, offshore Nigeria. Paper Arma 10-139, prepared for presentation at the 44th US Rock mechanics Symposium and 5th US-Canada Rock mechanics Symposium, Salt Lake City, June 27-30, 2010.
  19. M. Zwaan, R. Hartmans, S. Schoofs, B.R. de Zwart, G. Rocco, R. Adawi, F. Saadi, K. Shuaili, J. Lopez, J. Ita, T. L'Homme, T. Sorop, Y. Qiu, P.J. van den Hoek, F. Al-Kindy, S. Busaidi, and J. Fraser. EOR Field Management Through Well-Planned Surveillance. SPE 154620, presented at the SPE EOR Conference at Oil and Gas West Asia, Muscat, Oman, 16-18 April 2012.
  20. A. Petrik and P.J. van den Hoek, Multi-zone Waterflood Top Seal Integrity Assurance: insights from advanced Pressure Fall Off analysis using Smart Well and DTS technologies offshore Sakhalin, Russia. SPE-181985, presented at the SPE Russian Petroleum Technology Conference and Exhibition held in Moscow, Russia, 24–26 October 2016.
  21. Dougherty, R.L. & Abou-Sayed, A.S., Evaluation of the influence of in-situ reservoir conditions on the geometry of hydraulic fractures using a 3D simulator. SPE 13275 (1984).
  22. Meyer, B.R., Three-dimensional hydraulic fracturing simulation on personal computers: Theory and comparison studies. SPE 19239 (1989).
  23. Advani, S.H., Khattab, H. & Lee, J.K., Hydraulic fracture geometry modelling predictions and comparisons. SPE 13863 (1985).
  24. Bouteica, M.J., Hydraulic fracturing model based on a 3-D closed form: tests, analysis of fracture geometry and containment. J. SPEPE, November 1988, p. 445.
  25. Cleary, M.P., Barr, D.T. & Willis, R.M., Enhancement of real-time hydraulic fracturing models with full 3-D simulation. SPE 17713 (1988).
  26. Van den Hoek, P.J. Dimensions and Degree of Containment of Waterflood-Induced Fractures from Pressure Transient Analysis, SPERE, October 2005, 377-387.